Iris recognition using score fusion that combines pure biometrics and an auxiliary descriptor based on Shannon entropy with a rotation compensation mechanism using bit shifting[*]

Abdoul Kamal ASSOUMA[1,*], Tahirou DJARA[1], Yannick Kpatagnon EZIN[1], Sègniho Akpéni Majuste DONGBEHOUNDE[1], Olatundé Hilary Mélina BOCO[1]

[1] *Université d'Abomey-Calavi*

Abstract

This paper proposes an advanced hybrid approach to iris recognition, aimed at enhancing the robustness of biometric systems against eye rotations, lighting variations, and texture degradation. The method is based on a comprehensive pipeline that integrates CLAHE preprocessing, precise segmentation, normalization according to Daugman's Rubber Sheet model, and feature extraction based on multi-resolution 2D Gabor filters. The main innovation lies in the multimodal fusion of scores combining pure biometrics (IrisCode) with an **auxiliary textural descriptor based on global entropy**, coupled with a rotation compensation mechanism using bit shifting. Experimental results obtained on the MMU dataset demonstrate a significant improvement in performance, with an equal error rate of EER≈3,54 % after optimization.

Keywords

Shannon entropy, CLAHE, 2D Gabor filters, IrisCode, MMU dataset.

1. Introduction

Iris biometrics is recognized as one of the most reliable identification techniques due to the rich texture and stability of iris patterns [1], [2], [3]. Each human iris has a unique pattern, which forms as early as the seventh month of gestation and remains stable throughout life. This uniqueness, combined with the difficulty of artificially replicating it, makes it a particularly robust authentication method [4], [5].

However, existing systems remain susceptible to disturbances such as noise caused by eyelashes, eyelids, and light reflections, as well as rotations of the optical axis during acquisition [6]. To address these limitations, this paper proposes an optimized approach based on the following contributions:

- optimization of preprocessing through adaptive contrast enhancement and masking of noisy areas,
- implementation of a dynamic bit-shifting matching mechanism for rotation compensation,
- introduction of a hybrid fusion score combining Gabor filters and an auxiliary descriptor.

[*]CITA 2026 – Land, Smart Cities, and Sustainable Development, 25-26 June 2026, Cotonou, Benin

[1,*]Corresponding author.

abdoulk1@hotmail.com (A. K. ASSOUMA); csm.djara@gmail.com (T. DJARA) ; yannickkpatagnonezin@gmail.com (Y. K. EZIN); dmsa24program@gmail.com (S. A. M. DONGBEHOUNDE); melinaboco4@gmail.com (O. H. M. BOCO).

0000-0002-8591-6610 (T. DJARA)

2. Literary review

2.1. Iris Recognition: Basic Pipeline

An iris recognition system relies on a processing chain structured into several successive stages, ranging from the acquisition of the eye image to the authentication decision. This section describes this basic pipeline after iris acquisition.

2.1.1. Segmentation and Normalization

The first step involves isolating the iris region in the raw eye image. The circular contours of the pupil and limbus are detected using the circular Hough transform applied after gradient detection. At the same time, a binary mask identifies and excludes areas obscured by eyelashes, eyelids, and light reflections, which would otherwise introduce artifacts in subsequent steps.

The resulting image is then transformed into a rectangular representation with fixed dimensions using Daugman's Rubber Sheet model, which establishes a polar correspondence between the iris ring and a standardized strip, making the representation invariant to pupil dilation.

2.1.2. Feature Extraction and IrisCode Generation

The normalized image is analyzed using 2D multiresolution Gabor filters applied across multiple orientations and spatial scales. Each filtered response is binarized based on the sign of its real part, producing a compact binary code called the IrisCode. The use of multi-resolution filters captures the rich texture of the iris at different scales, giving the code good inter-individual discriminability.

2.1.3. Comparison and Decision Using Hamming Distance

The comparison phase measures the dissimilarity between the IrisCode of the person present and the one stored in the database using the normalized Hamming distance. A distance close to zero indicates a high degree of similarity (probable authentication), while a distance close to 0.5 is characteristic of two distinct, statistically independent irises.

2.2. Contribution of the auxiliary textural descriptor: Shannon entropy

While the base pipeline delivers good performance on controlled datasets, its limitations become apparent as soon as acquisition conditions deteriorate. Hamming distance alone is not always sufficient to distinguish pairs of imposters whose IrisCodes happen to be coincidentally similar. To address this vulnerability, the decision vector can be enriched with auxiliary descriptors: attributes that, when considered in isolation, do not uniquely identify an individual, but which, when combined with the primary biometric, enhance its robustness.

Among the possible auxiliary textural descriptors iris color, pupil shape, interocular distance Shannon entropy offers particularly well-suited properties. Derived from information theory, it quantifies the degree of complexity in the distribution of grayscale levels within an image. An iris with dense patterns (crypts, ridges, pigmented spots) exhibits high entropy, indicating a rich texture; conversely, a uniform or gradient image tends toward zero entropy.

This choice is based on three complementary properties. First, entropy is independent of the sensor and lighting conditions: it characterizes the structure of the grayscale levels without being affected by lighting conditions. Second, it is rotation-invariant: the pixel histogram does not change when the image is rotated, making it a global descriptor that is perfectly orthogonal to the bit-shifting mechanism. Third, it serves as an indicator of textural coherence: printed reproduction or a low-detail contact lens generates artificially low entropy, alerting the system to a potential fraud attempt.

When used as a textural consistency filter, Shannon entropy helps detect pairs whose IrisCodes appear similar by chance, but whose global complexity signatures are incompatible. This mechanism directly contributes to reducing the False Acceptance Rate (FAR).

2.3. Related Work

Iris recognition has been the subject of extensive research since Daugman's pioneering work in the early 1990s. This section reviews the most significant approaches, grouping them into three categories: feature extraction, degradation handling, and deep learning approaches,

2.3.1. Pioneering Work and Classical Approaches

Daugman [1], [3], [7] proposed the first comprehensive iris recognition system, based on 2D Gabor filters to encode the iris texture into a compact binary code called IrisCode. Hamming distance is used as a measure of dissimilarity between two codes. This system, still considered the gold standard in the field, achieves very low error rates on controlled databases.

Wildes [8] adopted a different approach based on Laplacian pyramid analysis and image correlation, rather than binary coding. Although more computationally intensive, this method demonstrates good robustness against variations in illumination. **Masek and Kovesi [9]**, for their part, implemented and released a complete processing pipeline in MATLAB, which is widely used as a benchmark in the scientific community.

Miron et al. [10] proposed a robust iris segmentation method based on a lightweight U-Net network, demonstrating good performance even in the presence of partial occlusions. **Sumi et al. [11]** conducted a comprehensive comparative evaluation of iris segmentation methods across several benchmark datasets, identifying the most robust approaches under real-world conditions.

2.3.2. Handling Degradation and Rotation

The sensitivity of systems to rotations of the optical axis is a well-documented problem. In Daugman's Rubber Sheet model, rotation of the head results in a simple horizontal shift in the normalized image. **Daugman [1]** describes a rotation compensation mechanism using circular shifting (bit-shifting): multiple alignments of the IrisCode are tested, and the one with the minimum Hamming distance is selected. **Li Ma et al. [12], [13]** have also developed a complementary method for extracting multi-resolution textural features, enhancing the ability to distinguish between individuals. This technique is now standard in most modern implementations. An alternative approach based on phase matching was proposed by **Miyazawa et al. [14], [15]**, offering comparable robustness against rotation variations.

Regarding obstructions caused by eyelashes and eyelids, several masking strategies have been proposed. **He et al. [16]** uses active contour models to precisely detect obstructed areas and exclude them from the similarity calculation. **Lei et al. [17]** proposed a lightweight dual-path fusion network for iris segmentation, offering a good trade-off between accuracy and computational efficiency.

2.3.3. Auxiliary Descriptors and Score Fusion

The concept of an auxiliary descriptor refers to the use of complementary features that, when considered in isolation, do not allow for unique identification but, when combined with a pure biometric, improve overall performance. **Jain et al. [18]** emphasize that the fusion of scores from heterogeneous sources is an effective general strategy for enhancing the performance of biometric systems compared to monomodal approaches.

Specifically, in the context of iris recognition, **Kumar and Passi [19]** have shown that a fusion strategy combining scores from several distinct iris matchers significantly improves authentication reliability compared to a single matcher. Shannon entropy, which quantifies the degree of textural complexity in an image, is a relevant robustness descriptor for characterizing the richness of iris patterns. Furthermore, **Yadav et al. [20]** specifically studied the impact of colored contact lenses on recognition systems, revealing the vulnerability of these systems to this type of fraud.

Building on this security research, **Tapia et al. [21]** proposed a liveness detection system based on a cascade of dedicated neural networks, capable of distinguishing a live iris from a presentation attack. Furthermore, **Yan et al. [22]** explored the multimodal fusion of ocular features to enhance recognition robustness, demonstrating the value of combining multiple sources of information beyond the iris alone. Finally, **Gupta et al. [23]** proposed a privacy-preserving iris recognition approach using federated learning, in which biometric data remains local and is never shared with a central server.

2.3.4. Deep Learning Approaches

Recent years have seen the emergence of convolutional neural networks (CNNs) applied to iris recognition. **Liu et al. [24]** propose DeepIris, a network that learns pairwise filter banks directly from iris data, enabling more robust heterogeneous verification without resorting to manually designed filters. **Nguyen et al. [25]** demonstrated that it is possible to leverage pre-trained CNN features without iris-specific retraining, while **Zhao and Kumar [26]** proposed learning deep spatial correspondences to improve discrimination. These approaches outperform traditional methods on large datasets but require a significant amount of training data and substantial computational resources.

A recent and comprehensive review of deep learning approaches applied to iris recognition was published by **Nguyen et al. [27]**, summarizing the major advances in the field. The introduction of Transformer architectures in this field has open up new possibilities: **Gao et al. [28]** proposed SwinIris, a system based on the Swin Transformer, achieving state-of-the-art performance on several datasets. Similarly, **Sun et al. [29]** proposes a Transformer framework specifically dedicated to iris recognition, leveraging attention mechanisms to better capture long-range textural patterns. **Wei et al. [30]** also proposed an approach aimed at improving the discriminability and robustness of iris recognition by explicitly modeling uncertainty factors during training. **Minaee et al. [31]**, for their part, provide a general overview of deep learning-based biometric recognition techniques, positioning the iris among the most effective modalities. **Yin et al. [32]**, meanwhile, offer a comprehensive review of deep learning methods applied to iris recognition, providing a consolidated view of the most recent state of the art.

Our approach differs from these studies by proposing an intermediate solution: it retains the interpretability and lightweight nature of classical methods (IrisCode + Gabor), while enhancing them with an auxiliary component (Shannon entropy) and dynamic rotation compensation, without resorting to deep learning. This approach is particularly well-suited to the constraints of the MMU dataset, which is characterized by intense reflections and frequent occlusions.

3. Proposed Methodology

The overall architecture of the proposed hybrid system is structured as shown in the block diagram in Figure 1. This image processing pipeline ensures a continuous flow of information from raw acquisition to the final decision.

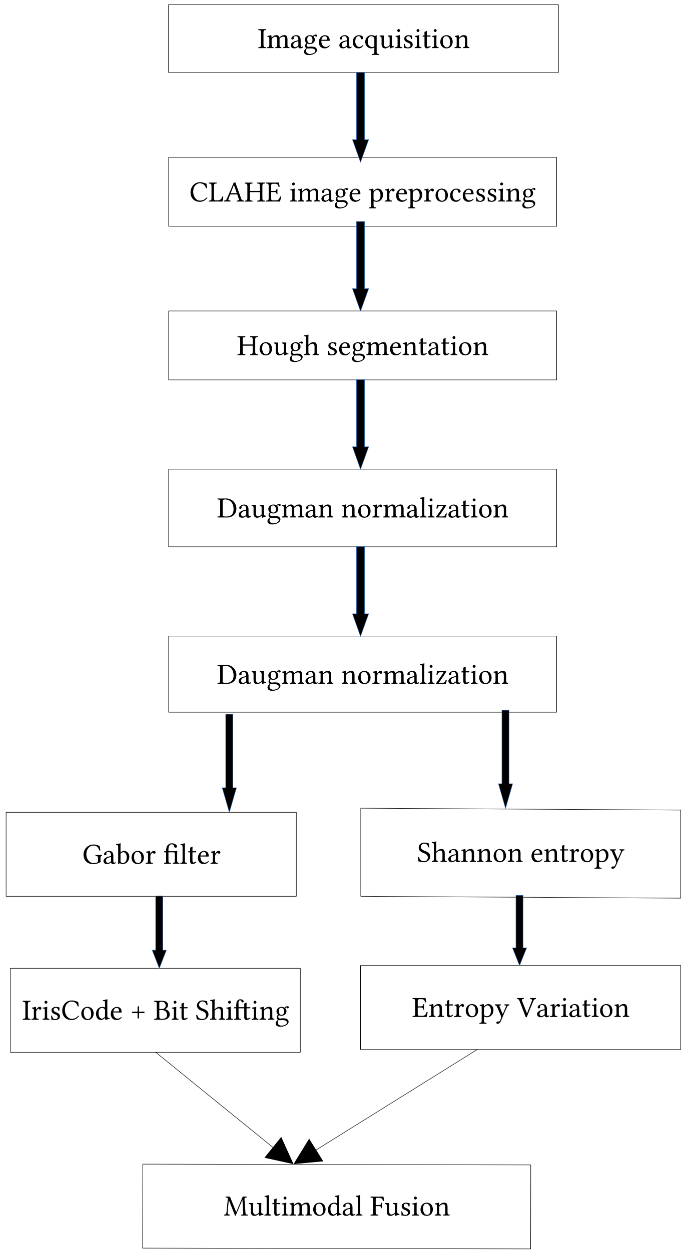

3.1. Preprocessing (CLAHE)

Unlike a traditional histogram equalizer, which flattens everything, CLAHE *(Contrast-Limited Adaptive Histogram Equalization)* operates locally on small rectangular regions called tiles (typically 8×8 or 16×16 pixels). Equalization is calculated independently for each tile, allowing local details—such as the iris crypts—to stand out, even if the lighting is not uniform across the entire eye. This equalization is calculated using the following local distribution formula:

$$g' = (L-1)\sum_{i=0}^{L} P(i)$$

Where P(i) is the cumulative distribution function of the grayscale levels in the tile in question.

Contrast Limitation (Clip Limit)

This is the “CL” in CLAHE. In standard equalization, if an area contains many pixels of the same color, the contrast is amplified excessively, causing noise (white/black specks) to appear.

- CLAHE defines a threshold (Clip Limit).
- If a bar in the histogram exceeds this threshold, the excess pixels are clipped and redistributed evenly across all other bars in the tile’s histogram.
- This prevents noise amplification while maintaining a natural contrast enhancement.

Bilinear Interpolation

If we stopped there, we would see squares (or “blocks”) in the image because each tile was processed differently. To eliminate these artificial edges, CLAHE uses **bilinear interpolation**. It blends the results from neighboring tiles so that brightness transitions are perfectly smooth.

Contrast Limitation: If a bar in the histogram exceeds a threshold (Clip Limit), the excess pixels are redistributed evenly across the entire histogram to avoid amplifying noise (very important for eyelashes in MMU).

3.2. Segmentation and Normalization (Rubber Sheet)

Segmentation involves detecting the circular contours of the pupil and iris using the circular Hough transform, applied after gradient detection. Occluded areas (eyelashes, eyelids, reflections) are identified and marked in a binary mask that is propagated throughout the pipeline.

Normalization adopts the Rubber Sheet model proposed by Daugman [1], which establishes a polar correspondence between the iris ring (between the pupil and the sclera) and a rectangle of fixed dimensions. This transformation makes the representation invariant to pupil dilation.

3.3. Feature Extraction (2D Gabor Filters)

2D multi-resolution Gabor filters are applied to the normalized image. The response of each filter is binarized (based on the sign of the real part) to produce the IrisCode. Using multiple orientations and scales allows us to capture the rich texture of the iris at different spatial resolutions.

3.4. Advanced Matching: Bit-Shifting (Rotation Compensation)

The eye is never perfectly straight. A head rotation of φ degrees results in a linear shift of *k* columns in the normalized ribbon. To correct this, the system calculates not just a single distance, but several, by circularly shifting the code:

$$C^s = C[(i+s) \bmod L]$$

The HD Hamming distance selected is the minimum obtained over a shift interval S = [-10, +10]:

$$HD_{min} = \left(\frac{\|(Code_A \, XOR \, Code^s{}_B) \cap (Mask_A \, XOR \, Mask^s{}_B)\|}{||(Mask_A \, XOR \, Mask_B)||} \right)$$

This mechanism ensures that even if the user tilts their head during acquisition, the system finds the best possible alignment of the patterns.

3.5. Shannon Entropy

Shannon entropy is used as an indicator of texture complexity.
In information theory, entropy measures the degree of uncertainty or disorder in a source of information. For an iris image, it quantifies the richness of the texture.

- Formula:

$$H = -\sum_{i=0}^{n-1} p(x_i) * \log_2(p(x_i))$$

Where $p(x_i)$ is the probability of a gray level *i* occurring.

In simple terms: An image that is entirely black or entirely white has an **entropy of 0** (total predictability, no information).
A rich iris with crypts, furrows, and spots has **high entropy** (great complexity, rich information).

➔ **Why this choice?**

There are other biometric modalities (iris color, pupil shape, interpupillary distance). But entropy is superior for three reasons:

- **Sensor independence:** Unlike color (which changes depending on lighting), entropy measures the structure of grayscale levels.
- **Rotation invariance:** Whether the iris is rotated by 10° or 90°, the pixel histogram remains the same, so the entropy does not change. This is the perfect complement to bit shifting.
- **Fraud detection:** A printed iris photo or a poorly made contact lens often has lower entropy than a real human eye due to the loss of detail during printing.

➔ **How does it play a role in recognition?**

In our system, entropy serves as a **consistency filter**. Imagine that two different irises (impostors) happen to have a low Hamming distance purely by chance.

- **Without Entropy:** The system might accept them (False Acceptance Rate, FAR).
- **With Entropy:** The system compares their complexity signatures. If iris A is very "smooth" (low entropy) and iris B is very "detailed" (high entropy), the system recognizes that they cannot be the same person, even if their binary codes are similar.

The Main Characteristics of Entropy in the Iris

- **Discrimination:** Two individuals rarely have the same texture distribution.
- **Stability:** For a given individual, iris entropy remains constant despite aging (unlike facial features).
- **Complementarity:** It provides **global** (statistical) information, whereas Gabor provides local (geometric) information.

3.6. Multimodal Fusion

Before multimodal fusion and subsequent classification, the raw scores from heterogeneous domains must be normalized. The minimum Hamming distance (HD_{min}) and the entropy variation
$(\Delta_{entropy} = |E_{entropy} - E_{entropy}|)$ are projected into the interval [0, 1] using robust Min-Max normalization according to the following equations. Note that the Hamming distance conventionally ranges from 0 to 0.5; to determine the entropy variation for our system, we

calculated the entropy difference between pairs in our system. We found an entropy variation ranging from 5.33 to 6.92. The scores are therefore normalized as follows:

- Hamming distance

$$HD_{norm} = \frac{HD_{min}}{0,5}$$

- Entropy change

$$\Delta E_{norm} = \frac{\Delta_{entropy} - 5,33}{6,92 - 5,33}$$

The fusion weight values were determined using an automated grid search procedure aimed at minimizing the equal error rate (EER). The optimal values selected are ***w1 = 0.30*** for the primary biometric and ***w2 = 0.70*** for the entropy descriptor. The final fused score is expressed as follows:

$$Score\,final = W1 * HD_{norm} + W2 * \Delta E_{norm}$$

where:

HD_{norm} the normalized Hamming distance obtained after rotation compensation.

ΔE_{norm} the normalized entropy difference between two iris images,

W1 and W2 are the weights assigned, respectively, to the Hamming distance obtained by pure biometrics and the entropy change between two iris images.

4. Experimental scenarios

The experiments were conducted using the MMU Iris Database, consisting of more than 45 subjects, each with 10 iris images taken from different positions, including 5 images of the left eye and 5 of the right eyes. It is characterized by the presence of intense reflections and partial obstructions, making segmentation particularly difficult. This resulted in 328 fully usable images, generating a total of **53.628 independent comparisons**, distributed as follows:

- **Authentic Pairs (Intra-class)**: 559 test combinations (comparisons of images from the same eye of the same subject).
- **Fake Pairs (Inter-class)**: 53,069 test combinations (cross-comparisons between different subjects).

The entire system was implemented in Java (JDK 17). The evaluation protocol follows the standard biometric protocol: for each subject, genuine pairs (same person) and impostor pairs (different people) are constructed [33]. Three main metrics are measured:

- **FAR (False Acceptance Rate):** the rate at which impostors are accepted.
- **FRR (False Rejection Rate):** the rate at which legitimate users are rejected (one legitimate user rejected).
- **EER (Equal Error Rate)**: the point of intersection where FAR = FRR, used as an overall performance metric.

5. Experimental results and discussions

5.1. Experimentals results

To accurately assess the individual contribution of each proposed technological block, an ablation study was conducted using three progressive scenarios based on the MMU dataset:

- **Scenario 1 (Simple IrisCode):** Extraction using Gabor filters and comparison using raw Hamming distance, without any rotation compensation or textural data.
- **Scenario 2 (IrisCode + Rotation):** Integration of the rotation compensation mechanism via circular bit shifting.
- **Scenario 3 (IrisCode + Rotation + Shannon):** Proposed comprehensive system integrating the linear fusion of the compensated Hamming score and the Shannon entropy differential

Table 1 presents the system's overall performance obtained on the MMU database for these different scenarios, along with the optimal threshold θ obtained for each after several comparison tests between individuals in the database.

Table 1. Overall system performance on the MMU database

Scenario	EER	FAR	FRR	Threshold (θ)	Database
Scenario 1	6.07%	5.90%	6.08%	0.553	MMU
Scenario 2	3.58%	3.68%	3.58%	0.534	MMU
Scenario 3	3.54%	3.31%	3.58%	0.160	MMU

Figure 2 illustrates the joint evolution of the False Acceptance Rate (FAR) and the False Rejection Rate (FRR) as a function of the decision threshold θ for each of the three scenarios studied. The projection of these curves highlights the direct impact of each technological block on class separability. It shows how the successive integration of the rotation compensation mechanism and entropy filtering restructures the error dynamics, shifting the Equal Error Rate (EER) point toward highly secure operating regions.

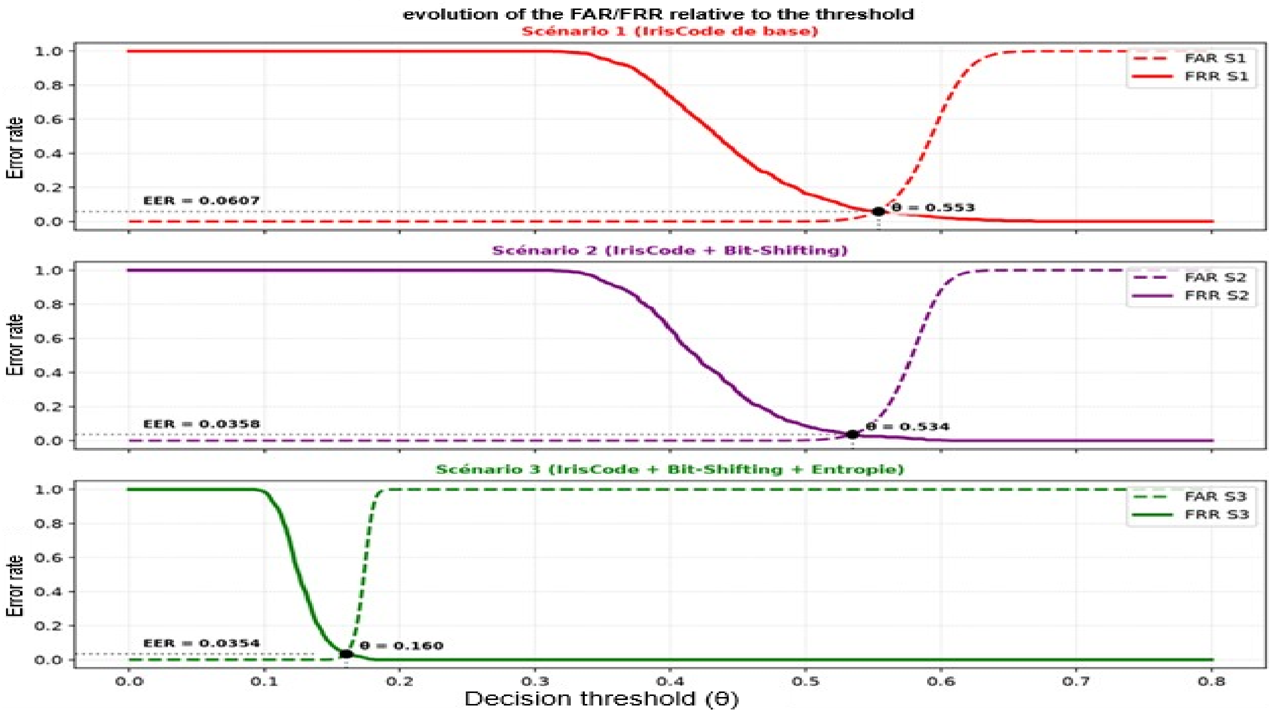

Figure 2: Joint evolution of the false acceptance rate (FAR) and false rejection rate (FRR) as a function of the decision threshold for the three scenarios studied.

*The absence of rotation compensation (**Scenario 1**) initially degrades system performance, resulting in an **EER of 6.07% (θ = 0.553)** due to frequent head tilts and slight geometric biases inherent in the MMU database capture conditions.*

*Enabling the bit-shifting mechanism (**Scenario 2)** effectively corrects these axial misalignments and significantly reduces the **EER to 3.58% (θ = 0.534)**, representing a net gain of 2.49% in overall accuracy, thereby validating the importance of robust compensation for angular variations in the iris.*

*Finally, the introduction of Shannon entropy as a filter for geometric coherence and algorithmic selection (**Scenario 3**) demonstrates its effectiveness by achieving a further improvement in performance. It enables the optimal **EER of 3.54%** to be reached. More precisely, the major contribution of entropy lies in the joint optimization of the system's security and robustness: it reduces the **false acceptance rate (FAR) to 3.31% (compared to 3.68% in Scenario 2)**. By eliminating coincidental matches between pairs of imposters (distinct iris textures but with locally similar patterns), this filtering allows for a tighter acceptance criterion. The optimal decision threshold (θ) is thus lowered to a much stricter and more secure value of **0.160** (compared to **0.534** previously), ensuring drastically increased immunity against intrusion attempts without compromising the false rejection rate (FRR).*

Although the study of operational thresholds allows us to determine the system's optimal operating point, it remains dependent on the application's configuration. To evaluate the intrinsic and overall performance of our classifier completely independently of the threshold, it is necessary to analyze its overall error trade-off.

To this end, Figure 3 presents the ROC curve comparing the discriminatory power of the three tested configurations:

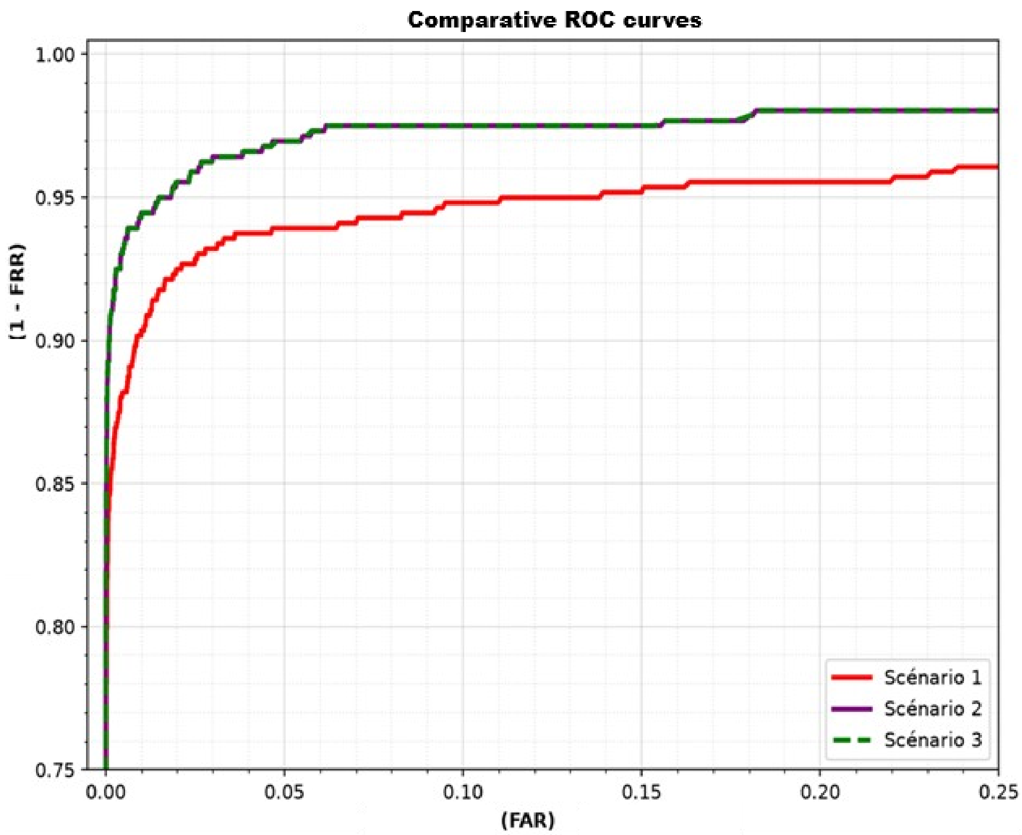

Figure 3: Comparative ROC curves for the three experimental scenarios on the MMU dataset

Table 2 presents an indicative comparison between our final system and methods from the literature that used similar datasets.

Table 2. Comparison with approaches from literature (EER, FAR, FRR)

Method / Approach	Database	EER (%)	FAR (%)	FRR (%)	Year
Daugman – IrisCode + Gabor [1]	CASIA	~0.1	~0.1	~0.2	2004
Masek & Kovesi – Gabor + Hamming [9]	CASIA	~5.0	~5.0	~5.0	2003
Kumar & Passi – Matcher fusion [19]	IITD	~3.0	~3.0	~3.5	2010
Yan et al. – Iris+periocular fusion [22]	CASIA-v4-dist	2.17	~2.0	~2.3	2024
Gao & Bourlai – SwinIris [28]	CASIA-IntervalV3	N/A	N/A	4.17	2024
Our Approach (Gabor + Entropy + Bit-Shift)	MMU	**~3.5**	**3.31**	**3.58**	**2026**

Methodological Note: *The direct numerical comparisons presented in Table 2 are purely indicative. Since state-of-the-art methods are evaluated on heterogeneous platforms (CASIA, IITD, MMU) characterized by radically different resolutions, sensors, and noise levels, a strict mathematical comparison of the EER is not scientifically fair. This table is intended solely to provide an order of magnitude for the performance of our approach relative to the standards in literature.*

5.2. Discussion

The achieved EER of 3.54% falls within the range of performance reported in the literature for modern iris recognition systems on real-world datasets with imperfect acquisition conditions. This result is particularly encouraging given the characteristics of the MMU dataset, which is known for its intense specular reflections and partial obstructions caused by eyelashes and eyelids.

Several factors account for this satisfactory performance. First, CLAHE preprocessing, with adaptive contrast limiting, helped stabilize illumination variations while preserving fine texture details. The bit-shifting mechanism, by testing multiple alignments over a range of ±10 shifts, effectively compensated for rotations of the optical axis, thereby reducing false rejections caused by variations in head posture during acquisition.

The use of Shannon entropy proved decisive in reducing false acceptances. By comparing the textural complexity profiles of the irises, the system was able to identify and reject pairs whose IrisCodes showed coincidental similarity, but whose entropy signatures were incompatible. This multimodal fusion strategy proved to be more robust than a monomodal approach relying solely on Hamming distance.

Despite these positive results, there are still several areas for improvement. First, segmentation using circular Hough transform, while functional, remains sensitive to intense reflections from the MMU dataset. Adopting segmentation using convolutional neural networks (UNet, SegNet) could improve contour detection accuracy and reduce normalization errors. Recent work supports this approach: Miron et al. demonstrated the effectiveness of a lightweight U-Net for iris segmentation in the presence of partial occlusions [10], while Lei et al. proposed a dual-path fusion network offering a good balance between accuracy and efficiency [17]. Furthermore, Sumi et al. conducted a comparative evaluation of segmentation methods across several benchmark datasets, providing useful benchmarks to guide future improvements [11]. Third, although the MMU dataset (45 subjects) presents relevant real-world acquisition challenges, its limited size constitutes a constraint for definitively validating the generalizability of the results. The absence of a cross-validation protocol on this preliminary version implies that the numerical performance metrics should be interpreted as proof of concept. A comprehensive evaluation on a second, larger-scale dataset, such as (CASIA-IrisV4, UBIRIS.v2[34]), is essential and constitutes the priority of our future work to confirm the model's robustness on a large scale. Datasets such as AFHIRIS [35] would also allow us to assess the fairness of the algorithm across African populations, which are often underrepresented in biometric evaluations.

Furthermore, it is important to highlight a methodological limitation regarding the determination of the optimal threshold $\theta = 0.16$. In this preliminary phase, the threshold was calculated and evaluated on the entire dataset, which introduces a minor risk of overfitting. To strengthen the system's generalization ability, our immediate work will incorporate a K-fold cross-validation protocol, which will allow for a strict separation between the threshold training subsets and the biometric test subsets.

6. Conclusion

This paper presented a hybrid approach to iris recognition, combining a conventional processing pipeline (CLAHE, Rubber Sheet, Gabor filters) with two innovations: a rotation compensation mechanism using bit shifting and an auxiliary textural component based on Shannon entropy. The system, implemented in Java and evaluated on the MMU database, achieves an EER of 3.54% with a decision threshold of 0.160.

These results demonstrate the effectiveness of multimodal fusion and confirm that combining pure biometrics (IrisCode) with an auxiliary descriptor (Shannon entropy) significantly improves the system's robustness under imperfect acquisition conditions. Dynamic rotation compensation via bit-shifting proved particularly effective at reducing false rejections, while entropy filtering helped limit random false acceptances.

Areas for improvement include: (1) adopting a more robust segmentation method based on convolutional neural networks (UNet, SegNet) to handle intense reflections more accurately, (2) automatic optimization of fusion weights via evolutionary search methods, (3) evaluation on larger and more diverse datasets (CASIA-IrisV4, UBIRIS.v2) to confirm the generalizability of the results, and (4) hardware optimization for real-time embedded applications.

Declaration on Generative AI

During the preparation of this work, the authors used chatGPT-5 mini for the following activities: language refinement, grammar corrections, and occasional structural suggestions. After using this tool, the authors reviewed and edited all generated content as needed and take full responsibility for the publication's scientific integrity and content.

References

[1] J. Daugman, "How Iris Recognition Works," IEEE Trans. Circuits Syst. Video Technol., vol. 14, no. 1, pp. 21–30, Jan. 2004, doi: 10.1109/TCSVT.2003.818350.

[2] L. Flom and A. Safir, "Iris recognition system," US4641349A, Feb. 3, 1987. Accessed Jan. 9, 2026. [Online]. Available at: https://patents.google.com/patent/US4641349A/en

[3] J. G. Daugman, "High confidence visual recognition of persons by a test of statistical independence," IEEE Trans. Pattern Anal. Machine Intell., vol. 15, no. 11, pp. 1148–1161, Nov. 1993, doi: 10.1109/34.244676.

[4] J. Daugman, "Probing the Uniqueness and Randomness of IrisCodes: Results From 200 Billion Iris Pair Comparisons," Proc. IEEE, vol. 94, no. 11, pp. 1927–1935, Nov. 2006, doi: 10.1109/JPROC.2006.884092.

[5] J. Daugman, "Statistical Richness of Visual Phase Information: Update on Recognizing Persons by Iris Patterns," International Journal of Computer Vision, vol. 45, no. 1, pp. 25–38, Oct. 2001, doi: 10.1023/A:1012365806338.

[6] K. W. Bowyer, K. Hollingsworth, and P. J. Flynn, "Image Understanding for Iris Biometrics: A Survey," Computer Vision and Image Understanding, vol. 110, no. 2, pp. 281–307, May 2008, doi: 10.1016/j.cviu.2007.08.005.

[7] J. G. Daugman, "Biometric personal identification system based on iris analysis," US5291560A, March 1, 1994. Accessed February 18, 2026. [Online]. Available at: https://patents.google.com/patent/US5291560A/en

[8] R. P. Wildes, "Iris recognition: an emerging biometric technology," Proc. IEEE, vol. 85, no. 9, pp. 1348–1363, Sept. 1997, doi: 10.1109/5.628669.

[9] Libor Masek and Peter Kovesi, "MATLAB Source Code for a Biometric Identification System Based on Iris Patterns," The University of Western Australia, Technical Report, 2003.

[10] C. Miron, A. Pasarica, V. Manta, and R. Timofte, "Efficient and Robust Iris Segmentation from Eye Images Using a Lightweight U-Net Convolutional Network," Multimed Tools Appl, vol. 81, no. 11, pp. 14961–14977, May 2022, doi: 10.1007/s11042-022-12212-8.

[11] M. R. Sumi, P. Das, A. Hossain, S. Dey, and S. Schuckers, "A Comprehensive Evaluation of Iris Segmentation on Benchmarking Datasets," Sensors, vol. 24, no. 21, p. 7079, Nov. 2024, doi: 10.3390/s24217079.

[12] Li Ma, Tieniu Tan, Yunhong Wang, and Dexin Zhang, "Personal Identification Based on Iris Texture Analysis," IEEE Trans. Pattern Anal. Machine Intell., vol. 25, no. 12, pp. 1519–1533, Dec. 2003, doi: 10.1109/TPAMI.2003.1251145.

[13] L. Ma, T. Tan, Y. Wang, and D. Zhang, "Efficient Iris Recognition by Characterizing Key Local Variations," IEEE Trans. on Image Process., vol. 13, no. 6, pp. 739–750, June 2004, doi: 10.1109/TIP.2004.827237.

[14] K. Miyazawa, K. Ito, T. Aoki, K. Kobayashi, and H. Nakajima, "An efficient iris recognition algorithm using phase-based image matching," in IEEE International Conference on Image Processing 2005, Genoa, Italy: IEEE, 2005, p. II–49. doi: 10.1109/ICIP.2005.1529988.

[15] K. Miyazawa, K. Ito, T. Aoki, K. Kobayashi, and H. Nakajima, "An effective approach for iris recognition using phase-based image matching," IEEE Trans. Pattern Anal. and Mach. Intell., vol. 30, no. 10, pp. 1741–1756, Oct. 2008, doi: 10.1109/TPAMI.2007.70833.

[16] Zhaofeng He, Tieniu Tan, Zhenan Sun, and Xianchao Qiu, "Toward Accurate and Fast Iris Segmentation for Iris Biometrics," IEEE Trans. Pattern Anal. Mach. Intell., vol. 31, no. 9, pp. 1670–1684, Sept. 2009, doi: 10.1109/TPAMI.2008.183.

[17] S. Lei, A. Shan, B. Liu, Y. Zhao, and W. Xiang, “Lightweight and efficient dual-path fusion network for iris segmentation,” Sci Rep, vol. 13, no. 1, p. 14034, Aug. 2023, doi: 10.1038/s41598-023-39743-w.

[18] A. K. Jain, A. Ross, and S. Prabhakar, “An Introduction to Biometric Recognition,” IEEE Trans. Circuits Syst. Video Technol., vol. 14, no. 1, pp. 4–20, Jan. 2004, doi: 10.1109/TCSVT.2003.818349.

[19] A. Kumar and A. Passi, “Comparison and Combination of Iris Matchers for Reliable Personal Authentication,” Pattern Recognition, vol. 43, no. 3, pp. 1016–1026, Mar. 2010, doi: 10.1016/j.patcog.2009.08.016.

[20] D. Yadav, N. Kohli, J. S. Doyle, R. Singh, M. Vatsa, and K. W. Bowyer, “Unraveling the Effect of Textured Contact Lenses on Iris Recognition,” IEEE Trans. Inform. Forensic Secur., vol. 9, no. 5, pp. 851–862, May 2014, doi: 10.1109/TIFS.2014.2313025.

[21] J. E. Tapia, S. Gonzalez, and C. Busch, “Iris Liveness Detection Using a Cascade of Dedicated Deep Learning Networks,” IEEE Trans. Inform. Forensic Secur., vol. 17, pp. 42–52, 2022, doi: 10.1109/TIFS.2021.3132582.

[22] Z. Yan, Y. Wang, K. Zhang, Z. Sun, and L. He, “Boosting Multi-modal Ocular Recognition via Spatial Feature Reconstruction and Unsupervised Image Quality Estimation,” Mach. Intell. Res., vol. 21, no. 1, pp. 197–214, Feb. 2024, doi: 10.1007/s11633-023-1415-y.

[23] H. Gupta, T. Rajput, R. Vyas, O. Vyas, and A. Puliafito, “Biometric Iris Identifier Recognition with Privacy-Preserving Mechanisms: A Federated Learning Approach,” 2023, pp. 493–504. doi: 10.1007/978-981-99-1648-1_41.

[24] N. Liu, M. Zhang, H. Li, Z. Sun, and T. Tan, “DeepIris: Learning a pairwise filter bank for heterogeneous iris verification,” Pattern Recognition Letters, vol. 82, pp. 154–161, Oct. 2016, doi: 10.1016/j.patrec.2015.09.016.

[25] K. Nguyen, C. Fookes, A. Ross, and S. Sridharan, “Iris Recognition With Off-the-Shelf CNN Features: A Deep Learning Perspective,” IEEE Access, vol. 6, pp. 18848–18855, 2018, doi: 10.1109/ACCESS.2017.2784352.

[26] Z. Zhao and A. Kumar, “Towards More Accurate Iris Recognition Using Deeply Learned Spatially Corresponding Features,” in 2017 IEEE International Conference on Computer Vision (ICCV), Venice: IEEE, Oct. 2017, pp. 3829–3838. doi: 10.1109/ICCV.2017.411.

[27] K. Nguyen, H. Proença, and F. Alonso-Fernandez, “Deep Learning for Iris Recognition: A Survey,” ACM Comput. Surv., vol. 56, no. 9, pp. 1–35, Oct. 2024, doi: 10.1145/3651306.

[28] R. Gao and T. Bourlai, “On Designing a SwinIris Transformer-Based Iris Recognition System,” IEEE Access, vol. 12, pp. 30723–30737, 2024, doi: 10.1109/ACCESS.2024.3369035.

[29] X. Sun, C. Wang, Y. Wang, J. Wei, and Z. Sun, “IrisFormer: A Dedicated Transformer Framework for Iris Recognition,” IEEE Signal Process. Lett., vol. 32, pp. 431–435, 2025, doi: 10.1109/LSP.2024.3522856.

[30] J. Wei, H. Huang, Y. Wang, R. He, and Z. Sun, “Towards More Discriminative and Robust Iris Recognition by Learning Uncertain Factors,” IEEE Trans. Inform. Forensic Secur., vol. 17, pp. 865–879, 2022, doi: 10.1109/TIFS.2022.3154240.

[31] S. Minaee, A. Abdolrashidi, H. Su, M. Bennamoun, and D. Zhang, “Biometric Recognition Using Deep Learning: A Survey,” Artif Intell Rev, vol. 56, no. 8, pp. 8647–8695, Aug. 2023, doi: 10.1007/s10462-022-10237-x.

[32] Y. Yin, S. He, R. Zhang, H. Chang, and J. Zhang, “Deep learning for iris recognition: a review,” Neural Comput & Applic, vol. 37, no. 17, pp. 11125–11173, June 2025, doi: 10.1007/s00521-025-11109-5.

[33] “Information technology—Biometric data interchange formats—Part 6: Iris image data,” ISO/IEC Standard 19794–6:2011, 2011.

[34] H. Proença and L. A. Alexandre, “UBIRIS: A Noisy Iris Image Database,” in Image Analysis and Processing – ICIAP 2005, vol. 3617, F. Roli and S. Vitulano, eds., in Lecture Notes in Computer Science, vol. 3617. , Berlin, Heidelberg: Springer Berlin Heidelberg, 2005, pp. 970–977. doi: 10.1007/11553595_119.
[35] O. N. Akande, N. Ojimba, O. Atele, O. C. Abikoye, and A. Akindele, “AFHIRIS: African Human Iris Dataset (Version 1),” vol. 1, May 2022, doi: 10.17632/r3ypmmp2gs.1.